IEEE Access
Multidisciplinary | Rapid Review | Open Access Journal

Received September 22, 2019, accepted October 15, 2019, date of publication October 18, 2019, date of current version October 30, 2019.

Digital Object Identifier 10.1109/ACCESS.2019.2948229

Robust Partially Strong Tracking Extended Consider Kalman Filtering for INS/GNSS Integrated Navigation

TAI-SHAN LOU, NAN-HUA CHEN, ZHI-WU CHEN, AND XIAO-LEI WANG
School of Electric and Information Engineering, Zhengzhou University of Light Industry, Zhengzhou 45002, China

Corresponding author: Zhi-Wu Chen (chenyyj@163.com)

This work was supported in part by the Key Science and Technology Program of Henan Province under Grant 182102210177 and Grant 192102310185, in part by the Maker Space Incubation Project under Grant 2018ZCKJ308, in part by the Graduate Technology Innovation Fund Project of Zhengzhou University of Light Industry under Grant 2018043, in part by the Key Research Projects of Henan Higher Education Institutions under Grant 18A413003, and in part by the Science and Technology Innovation Team Project of Henan Province University under Grant 19IRTSTHN013.

ABSTRACT Unknown biases or perturbations in the INS/GNSS integrated navigation system may produce unforeseeable negative effects when the navigation states are estimated by using the Kalman filtering and its variants. To mitigate these undesirable effects in the INS/GNSS integrated navigation, a novel partially strong tracking extended consider Kalman filtering (PSTECKF) is proposed. In the presented PSTECKF algorithm, the biases are not estimated, but their covariance and co-covariance are incorporated into the state estimation covariance by using a nonlinear "consider" approach. Based on the above, the PSTECKF also partially introduces an adaptive fading factor into the predicted covariance of the states, which excludes the co-covariance between the states and biases, to compensate the nonlinear approximation errors and navigation system covariance uncertainties. Simulation results demonstrate the performance of the proposed PSTECKF for INS/GNSS integrated navigation is superior to that of the EKF and ECKF when the biases or perturbations happen in a navigation system.

INDEX TERMS INS/GNSS integrated navigation, consider Kalman filter, adaptive filtering, bias, strong tracking.

I. INTRODUCTION

The inertial navigation system (INS) and global navigation satellite system (GNSS) integrated navigation system organically merge advantages of two sensors, which are the high short-term navigation accuracy of INS and high long-term navigation accuracy of GNSS, and have a widely application in navigation and positioning field [1]–[5]. The INS/GNSS integrated navigation system overcomes the limitations of using INS or GNSS navigation systems alone and can work well in all weather conditions around the world. When the states of the INS/GNSS integrated navigation system are estimated by using the Kalman filtering and its variants, there are two methods can be selected, which are the direct method and the indirect method [6]. The indirect method obtains the optimal estimations of the navigation errors of the INS and GNSS by utilizing the navigation errors as the system states. The direct method directly gives the optimal estimations of the integrated navigation parameters by using filtering algorithm, and its states are the output navigation parameters of the navigation system. Comparing to the indirect method, the direct method has two advantages: one is more accurately propagating the navigation states and another is avoiding double counting by using mechanical calibration equation of the INS [7]–[9].

To utilize the direct method for the INS/GNSS integrated navigation system needs to solve some key technology problems, such as model nonlinearity, drifts of the inertial measurement unit (IMU), biases of the system and perturbations of the whole navigation system [6], [10]. Many methods are proposed to solve above problems for the directly integrated navigation system. One strategy is using more accuracy nonlinear algorithm to take place of the extended Kalman filter (EKF) [3], [5], [11]. Crassidis utilized the unscented Kalman filter (UKF) to estimate the position /attitude of the INS and global positioning system (GPS) by approximating a Gaussian distribution, and obtained more precise navigation states than the EKF [4]. Sun and Tang combined cubature Kalman

The associate editor coordinating the review of this manuscript and approving it for publication was Zhixiong Peter Li.

filter and particle filter to deal with the large initial condition errors in the INS/GPS integrated navigation system [12]. Another strategy is adaptive or robust strategy for the uncertainties in the navigation system. For the uncertain noises, many filtering algorithms have been proposed to mitigate their negative effects in INS/GNSS integration, such as strong tracking filtering [9], [10], covariance matching UKF [8], fuzzy adaptive filtering [13]–[15]. For the drifts of the IMU, they are always augmented into the system states to estimate together for the INS/GNSS integrated navigation system. Kim et al. proposed an adaptive two-stage EKF to deal with the unknown fault biases in INS/GPS loosely coupled system [16]. George and Sukkarieh augmented the biases of the IMU and the clock biases of the GPS into the state vector to estimate and improved the navigation accuracy for the tightly coupled INS/GPS integration of unmanned aerial vehicle (UAV) [17]. Zhao et al. designed a robust Kalman filter to solve the exogenous disturbances, device damage and inaccurate sensor noise statistics in the loosely coupled INS/GPS navigation system [18]. So, mitigating the negative effects of the nonlinearity, drifts, biases and perturbations of the navigation system to improve the navigation accuracy becomes necessary.

To compensate the biases, a consider Kalman filtering (CKF), which is also called Schmidt-Kalman filtering, have been proposed [19] and used in Mars entry navigation [20], [21], target tracking [22], [23], spacecraft attitude estimation [24], [25], and so on. The CKF incorporates the covariance of the biases into the state estimation covariance, and not directly estimate them. This handling method about the biases could consider the effects of the biases and reduce the computation cost by not estimating them. Then, many modified CKF are proposed to improve estimation accuracy, such as unscented CKF [26], norm-constrained CKF [24], multiple adaptive fading CKF [27], ensemble CKF [25], Gaussian mixture CKF [28].

This paper proposed a partially strong tracking extended consider Kalman filtering (PSTECKF) to overcome the navigation system model uncertainties and mitigate the negative effects of the biases in INS/GNSS integrated navigation system. Based on the extended consider Kalman filtering (ECKF), the PSTECKF does not estimate the biases, and only incorporates their covariance and co-covariance into the state estimation covariance by using the "consider" approach proposed by Schmidt [19]. Then, the PSTECKF partially introduces a suboptimal adaptive fading factor into the predicted covariance to compensate the model nonlinear approximation errors and navigation system covariance uncertainties.

The remainder of this paper is organized as follows. In Section 2, the mathematical model for INS/GNSS integrated navigation system is introduced. The extended consider Kalman filter algorithm is introduced in Section 3. Section 4 derives the partially strong tracking extended consider Kalman filtering algorithm. In Section 5, simulations are carried out to evaluate the performance of the proposed approach. Finally, conclusions are shown in the end.

II. INS/GNSS INTEGRATION NAVIGATION SYSTEM

The basic principle of the INS/GNSS integration is to use the position and velocity information of the GNSS to correct the position and velocity of INS [2], [29]. In the direct filtering method, the dynamic model of INS/GNSS integration is established by using the inertial navigation equations and the IMU error equations. The measurement model is constructed by using the output information of velocity and position from GNSS [7], [10], [30].

A. KINEMATIC MODEL

The INS/GNSS integrated navigation scheme consists of the IMU, which provides specific forces of three axes, and the GNSS, which provides the position and velocity information in the East-North-Up (E-N-U) geographic coordinate frame. The direct integrated navigation system is modeled to directly describe the navigation parameters by using the information of the IMU. Considering the constant drifts of the gyroscope and accelerometer, the navigation system state vector is defined as

$$x = \left[\phi_e \ \phi_n \ \phi_u \ v_e \ v_n \ v_u \ \varphi \ \lambda \ h \ \varepsilon_e \ \varepsilon_n \ \varepsilon_u \ \Delta_e \ \Delta_n \ \Delta_u \right]^T \quad (1)$$

and the dynamic equation of the INS/GNSS integrated navigation system is given by [7], [10]

$$\begin{cases}
\dot{\phi}_e = \dfrac{v_n \delta h}{(R_M+h)^2} - \dfrac{\delta v_n}{(R_M+h)} + (\omega_{ie}\sin\varphi + \dfrac{v_e \tan\varphi}{R_N+h})\phi_n \\
\quad -(\omega_{ie}\cos\varphi + \dfrac{v_e}{R_N+h})\phi_u + \varepsilon_e \\
\dot{\phi}_n = -\dfrac{\delta h}{(R_N+h)^2} v_e - \omega_{ie}\sin\varphi\delta\varphi + \dfrac{\delta v_e}{(R_N+h)} \\
\quad -(\omega_{ie}\sin\varphi + \dfrac{v_e\tan\varphi}{R_N+h})\phi_e - \dfrac{v_n}{R_M+h}\phi_u + \varepsilon_n \\
\dot{\phi}_u = -(\dfrac{\tan\varphi\delta h}{(R_N+h)^2} - \dfrac{\sec^2\varphi\delta\varphi}{R_N+h})v_e \quad + \omega_{ie}\cos\varphi\delta\varphi \\
\quad + \dfrac{\delta v_e \tan\varphi}{(R_N+h)} \\
\quad +(\omega_{ie}\cos\varphi + \dfrac{v_e}{R_N+h})\phi_e + \dfrac{v_n}{R_M+h}\phi_n + \varepsilon_u \\
\dot{v}_e = (\dfrac{v_e\tan\varphi}{R_N+h} + 2\omega_{ie}\sin\varphi)v_n \\
\quad -(2\omega_{ie}\cos\varphi + \dfrac{v_e}{R_N+h})v_u \\
\quad -f_u\phi_n + f_n\phi_u + f_e + \Delta_e \\
\dot{v}_n = -(2\omega_{ie}\sin\varphi + \dfrac{v_e\tan\varphi}{R_N+h})v_e - \dfrac{v_n v_u}{R_M+h} \\
\quad +f_u\phi_e - f_e\phi_u + f_n + \Delta_n \\
\dot{v}_u = (2\omega_{ie}\cos\varphi + \dfrac{v_e}{R_N+h})v_e + \dfrac{v_n^2}{R_M+h} \\
\quad -f_n\phi_e + f_e\phi_n + f_u - g + \Delta_u \\
\dot{\varphi} = \dfrac{v_n}{R_M+h} \\
\dot{\lambda} = \dfrac{v_e}{(R_N+h)\cos\varphi} \\
\dot{h} = v_u \\
\dot{\varepsilon}_e = \omega_{\varepsilon_e}, \quad \dot{\varepsilon}_n = \omega_{\varepsilon_n}, \ \dot{\varepsilon}_u = \omega_{\varepsilon_u} \\
\dot{\Delta}_e = \omega_{\Delta_e}, \quad \dot{\Delta}_n = \omega_{\Delta_n}, \ \dot{\Delta}_u = \omega_{\Delta_u}
\end{cases} \quad (2)$$

where ϕ_e, ϕ_n and ϕ_u are attitude error angles of mathematics platform; v_e, v_n and v_u are the velocities in the E-N-U directions; φ, λ and h are respectively latitude, longitude and altitude; $[\varepsilon_e, \varepsilon_n, \varepsilon_u]^T$ and $[\Delta_e, \Delta_n, \Delta_u]^T$ are the constant drift of the gyroscope and acceleration, respectively. δv_e and δv_n are the velocity differences between the INS and the GNSS in the east and north directions, respectively; $\delta\varphi$ and δh are the latitude and height difference between the INS and the GNSS, respectively; f_e, f_n and f_u are the specific forces of the accelerometer in the E-N-U directions. The noise vector $[\varepsilon_e, \varepsilon_n, \varepsilon_u, \Delta_e, \Delta_n, \Delta_u]^T$ is random errors coming from the gyroscope and the accelerometer.

Considering the state perturbations of the UAV, such as model uncertainties or gust, the integrated navigation system model is following as [9], [10]

$$\dot{x} = f(x, p_1) + w \tag{3}$$

where $f(\cdot)$ is a nonlinear function, p_1 is the perturbation vector or bias vector and $w = [0_{1\times 9}, [\varepsilon_e, \varepsilon_n, \varepsilon_u], [\Delta_e, \Delta_n, \Delta_u]]^T$ is the process noise vector.

B. MEASUREMENT MODEL

The GNSS receiver can provide the velocity and position of the UAV, and this information is taken as the measurements [7], [10]. However, the measurements of the GNSS have many system biases, such as satellite dock biases, ephemeris biases, receiver clock offset, ionospheric delay biases, tropospheric delay biases and multi-path biases. These biases determine the accuracy of the GNSS and then will affect the navigation accuracy [1], [6].

Considering the above biases of the GNSS, the measurement model of the INS/GNSS integrated navigation system is given by:

$$z = h(x) + p_2 + v \tag{4}$$

where the linear function $h(x) = [v_{ge}, v_{gn}, v_{gu}, \varphi_g, \lambda_g, h_g]^T$ is the carrier velocity and position measured by the GNSS; $p_2 = [b_{vge}, b_{vgn}, b_{vgu}, b_{pge}, b_{pgn}, b_{pgu}]^T$ is the measurement bias vector; $v = [v_{vge}, v_{vgn}, v_{vgu}, v_{pge}, v_{pgn}, v_{pgu}]^T$ is the measurement noise vector, in which $[v_{vge}, v_{vgn}, v_{vgu}]^T$ and $[v_{pge}, v_{pgn}, v_{pgu}]^T$ are the random errors of the GNSS velocity measurement values and the GNSS position in the E-N-U directions, respectivly.

C. DISCRETE-TIME INTEGRATED NAVIGATION SYSTEM

Combing the process perturbation vector p_1 and the measurement bias vector p_2 as a vector $p = [p_1, p_2]^T$, the above continuous navigation system (3) and (4) are modified as

$$\dot{x} = f(x, p) + w \tag{5}$$
$$z = h(x, p) + v \tag{6}$$

Discretizing the above continuous INS/GNSS integration navigation system obtains the discrete-time equation as follows

$$x_k = f(x_{k-1}, p) + w_{k-1} \tag{7}$$
$$z_k = h(x_k, p) + v_k \tag{8}$$

where w_k and v_k are assumed to be independent process and measurement Gaussian white noise sequences with zero means and variances Q_k and R_k, respectively. These two parameters satisfy:

$$E[w_k w_j^T] = \begin{cases} Q_k, j = k \\ 0, j \neq k \end{cases};$$
$$E[v_k v_j^T] = \begin{cases} R_k, j = k \\ 0, j \neq k \end{cases};$$
$$E[w_k v_j^T] = 0 \quad \text{for all } j \text{ and } k \tag{9}$$

III. EXTENDED CONSIDER KALMAN FILTER

In this section, the derivation process and formula of the extended consider Kalman filter are briefly summarized to conveniently introduce the partially strong tracking ECKF.

In the above discrete-time INS/GNSS integration navigation system model (7) and (8), there are process perturbations and the measurement biases, which can be considered as uncertain parameters or biases. To mitigate the negative effects of the biases or uncertain parameters, a "consider" approach is presented to account for these uncertainties by incorporating their statistics property into the state estimate covariance and not estimating them [19], [20]. Based on the above idea, the ECKF is summarized by the expanding state method and a mandatory zero setting for the gain matrix.

To make the best of the uncertain biases in the Kalman filtering, some statistic assumptions and correlations between the biases and the state are set as

$$P_{pp} = Cov\{\delta p\} \tag{10}$$
$$C_k = E\left\{\tilde{x}_k \delta p^T\right\} \tag{11}$$

where P_{pp} is the covariance matrix of the biases; $\delta p = p - \bar{p}$ is the error between the bias vector p and its reference value $\bar{p}$; C_k is the cross-covariance matrix of the state estimation errors and the biases; $\tilde{x}_k = x_k - \hat{x}_k$ is the state estimation error.

As the EKF, the ECKF also uses the first-order Taylor series expansion method to approximate the nonlinear function. So, the nonlinear function $f(x_{k-1}, p)$ in Eq. (7) is expanded around the nominal state estimate $\hat{x}_{k-1}$ and the reference value $\bar{p}$, and simplified as follows:

$$\delta x_k = \Phi_{k/k-1}\delta x_{k-1} + \Psi_{k/k-1}\delta p + w_{k-1} \tag{12}$$

where $\delta x_k = x_k - \hat{x}_{k/k-1}$ and $\delta x_{k-1} = x_{k-1} - \hat{x}_{k-1}$. The linearized coefficient matrices $\Phi_{k/k-1}$and $\Psi_{k/k-1}$ are respectively given by

$$\Phi_{k/k-1} = \frac{\partial f(x_{k-1}, \bar{p})}{\partial x_{k-1}}\Big|_{x_{k-1}=\hat{x}_{k-1}} \tag{13}$$
$$\Psi_{k/k-1} = \frac{\partial f(x_{k-1}, \bar{p})}{\partial p_{k-1}}\Big|_{p=\bar{p}} \tag{14}$$

Similarly, the nonlinear measurement function $h(x_k, p)$ in Eq. (8) can be linearized around $\hat{x}_{k/k-1}$ and $\bar{p}$ as follows:

$$\delta z_k = H_k \delta x_k + N_k \delta p + v_k \tag{15}$$

where $\delta z_k = z_k - \hat{z}_{k/k-1}$, and $\hat{z}_{k/k-1} = h(\hat{x}_{k/k-1}, \bar{p})$. The linearized coefficient matrices H_k and N_k are respectively given by

$$H_k = \frac{\partial h(x_k, \bar{p})}{\partial x_k}\Big|_{x_k=\hat{x}_{k/k-1}} \tag{16}$$

$$N_k = \frac{\partial h(\hat{x}_{k/k-1}, \bar{p})}{\partial p}\Big|_{p=\bar{p}} \tag{17}$$

Considering the linearized discrete-time model in Eqs (12) and (15), the following results are obtained by extending the bias error vector δp to the state error vector δx_k following by

$$\begin{bmatrix} \delta x_k \\ \delta p \end{bmatrix} = \begin{bmatrix} \Phi_{k/k-1} & \Psi_{k/k-1} \\ 0 & I \end{bmatrix} \begin{bmatrix} \delta x_{k-1} \\ \delta p \end{bmatrix} + \begin{bmatrix} w_{k-1} \\ 0 \end{bmatrix} \tag{18}$$

$$\delta z_k = [H_k, N_k] \begin{bmatrix} \delta x_k \\ \delta p \end{bmatrix} + v_k \tag{19}$$

Based on the augmented system model Eqs. (18) and (19), the ECKF algorithm can be obtained as the standard Kalman filtering. The time update of the ECKF algorithm is follows by

$$\delta\hat{x}_{k/k-1} = \Phi_{k/k-1}\delta\hat{x}_{k-1} + \Psi_{k/k-1}\delta\hat{p} \tag{20}$$

$$\begin{bmatrix} P_{k/k-1} & C_{k/k-1} \\ C_{k/k-1}^T & P_{pp} \end{bmatrix} = \begin{bmatrix} \Phi_{k/k-1} & \Psi_{k/k-1} \\ 0 & I \end{bmatrix} \begin{bmatrix} P_{k-1} & C_{k-1} \\ C_{k-1}^T & P_{pp} \end{bmatrix} \begin{bmatrix} \Phi_{k/k-1} & \Psi_{k/k-1} \\ 0 & I \end{bmatrix}^T + \begin{bmatrix} Q_{k-1} & 0 \\ 0 & 0 \end{bmatrix} \tag{21}$$

and the measurement update is

$$\bar{K}_k = \begin{bmatrix} K_k \\ 0 \end{bmatrix} = \begin{bmatrix} P_{k/k-1} & C_{k/k-1} \\ C_{k/k-1}^T & P_{pp} \end{bmatrix} [H_k^T N_k^T] \left\{ [H_k, N_k] \begin{bmatrix} P_{k/k-1} & C_{k/k-1} \\ C_{k/k-1}^T & P_{pp} \end{bmatrix} \begin{bmatrix} H_k^T \\ N_k^T \end{bmatrix} + R_k \right\}^{-1} \tag{22}$$

$$\delta\hat{x}_k = \delta\hat{x}_{k/k-1} + K_k(\delta z_k - H_k\delta\hat{x}_{k/k-1} - N_k\delta\hat{p}) \tag{23}$$

$$\begin{bmatrix} P_k & C_k \\ C_k^T & P_{pp} \end{bmatrix} = \left\{ I - \begin{bmatrix} K_k \\ 0 \end{bmatrix} [H_k, N_k] \right\} \begin{bmatrix} P_{k/k-1} & C_{k/k-1} \\ C_{k/k-1}^T & P_{pp} \end{bmatrix} \tag{24}$$

where the gain matrix of the bias in $\bar{K}_k$ is forced to zero, because the ECKF only considers the variance statistical characteristics of the bias and does not estimate parameter δp.

Consider the error $\delta\hat{p} = 0$ and $\delta\hat{x}_{k-1} = 0$ in Eq. (20), $\Phi_{k/k-1}\delta\hat{x}_{k-1} + \Psi_{k/k-1}\delta\hat{p} = 0$ leads to $\delta\hat{x}_{k/k-1} = 0$, and simplify the ECKF algorithm in Eqs. (20)~(24). The whole algorithm of the ECKF is summarized as following:

Step 1: Initialize the state $\hat{x}_0$, the state covariance matrix P_0 and the cross-covariance variance C_0.

Step 2: Time update

$$\hat{x}_{k/k-1} = f(\hat{x}_{k-1}, \bar{p}) \tag{25}$$

$$P_{k/k-1} = \Phi_{k/k-1}P_{k-1}\Phi_{k/k-1}^T + \Phi_{k/k-1}C_{k-1}\Psi_{k/k-1}^T + \Psi_{k/k-1}C_{k-1}^T\Phi_{k/k-1}^T + \Psi_{k/k-1}P_{pp}\Psi_{k/k-1}^T + Q_{k-1} \tag{26}$$

$$C_{k/k-1} = \Phi_{k/k-1}C_{k-1} + \Psi_{k/k-1}P_{pp} \tag{27}$$

Step 3: Measurement update

$$K_k = (P_{k/k-1}H_k^T + C_{k/k-1}N_k^T)(H_kP_{k/k-1}H_k^T + N_kC_{k/k-1}^TH_k^T + H_kC_{k/k-1}N_k^T + N_kP_{pp}N_k^T + R_k)^{-1} \tag{28}$$

$$\hat{x}_k = \hat{x}_{k/k-1} + K_k\{z_k - h(\hat{x}_{k/k-1}, \bar{p})\} \tag{29}$$

$$P_k = (I - K_kH_k)P_{k/k-1} - K_kN_kC_{k/k-1}^T \tag{30}$$

$$C_k = (I - K_kH_k)C_{k/k-1} - K_kN_kP_{pp} \tag{31}$$

Note that the standard EKF algorithm can be obtained by setting $P_{pp} = 0$.

IV. PSTECKF ALGORITHM

To overcome the uncertainties in state-space system model and satisfy the accuracy and adaptability of the filtering, a mutually orthogonal principle of the predicted measurement residual sequences is proposed by Zhou and Frank [31] and Zhou *et al.* [32]. Based on the mutually orthogonal principle, a time-varying suboptimal adaptive fading factor is introduced into the predicted state error covariance matrix to adjust the gain matrix K_k in real time, and then improve the filtering precision [27], [32]. Here, to improve the robustness and adaptability of the ECKF, a suboptimal adaptive fading factor is partially introduced into in Eq. (26), which is different from the reference [27]. In the reference [27], a multiple fading factor is set on the whole augmented state, and the predicted state error covariance and the cross-covariance are adjusted at the same time. Here, only the predicted state error covariance is modified by a suboptimal adaptive fading factor, and the formula is

$$P_{k/k-1} = \lambda_k P_{k/k-1}^* + Q_{k-1} \tag{32}$$

where $P_{k/k-1}^* = \Phi_{k/k-1}P_{k-1}\Phi_{k/k-1}^T + \Phi_{k/k-1}C_{k-1}\Psi_{k/k-1}^T + \Psi_{k/k-1}C_{k-1}^T\Phi_{k/k-1}^T + \Psi_{k/k-1}P_{pp}\Psi_{k/k-1}^T$, λ_k is the suboptimal adaptive fading factor to be calculated.

Substituting Eq. (32) into Eq.(21) yields a new augmented prediction variance matrix

$$\begin{bmatrix} P_{k/k-1} & C_{k/k-1} \\ C_{k/k-1}^T & P_{pp} \end{bmatrix} = \begin{bmatrix} \lambda_k P_{k/k-1}^* & (\Phi_{k/k-1}C_{k-1} + \Psi_{k/k-1}P_{pp}) \\ (\Phi_{k/k-1}C_{k-1} + \Psi_{k/k-1}P_{pp})^T & P_{pp} \end{bmatrix} + \begin{bmatrix} Q_{k-1} & 0 \\ 0 & 0 \end{bmatrix} \tag{33}$$

According to the mutually orthogonal principle, the predicted measurement residual sequences $\tilde{z}_k = z_k - h(\hat{x}_{k/k-1}, p)$ must be kept orthogonal to each other. The residual sequences satisfy the following equation

$$E[\tilde{z}_{k+j}\tilde{z}_k^T] = 0, \quad k = 0, 1, 2\ldots\ldots, \ j{=}1, 2, 3\ldots\ldots \tag{34}$$

Substituting $\tilde{z}_k = z_k - h(\hat{x}_{k/k-1}, p)$ into Eq. (34) to obtain:

$$\begin{aligned} &E[\tilde{z}_{k+j}\tilde{z}_k^T] \\ &= [H_{k+j}, N_{k+j}] \begin{bmatrix} \Phi_{k+j-1/k+j-2} & \Psi_{k+j-1/k+j-2} \\ 0 & I \end{bmatrix} \\ &\quad \left\{I - \bar{K}_{k+j-1}[H_{k+j-1}, N_{k+j-1}]\right\} \cdots \begin{bmatrix} \Phi_{k+1/k} & \Psi_{k+1/k} \\ 0 & I \end{bmatrix} \\ &\quad \times \left\{I - \bar{K}_{k+1}[H_{k+1}, N_{k+1}]\right\} \begin{bmatrix} \Phi_{k/k-1} & \Psi_{k/k-1} \\ 0 & I \end{bmatrix} \Lambda_k, \\ &\quad j = 1, 2, 3, \cdots \end{aligned} \tag{35}$$

where Λ_k is

$$\Lambda_k = \begin{bmatrix} P_{k/k-1} & C_{k/k-1} \\ C_{k/k-1}^T & P_{pp} \end{bmatrix} \begin{bmatrix} H_k^T \\ N_k^T \end{bmatrix} - \bar{K}_k V_k \tag{36}$$

Substituting the optimal gain $\bar{K}_k$ into Eq. (36) to make $\Lambda_k = 0$, and also $E[\tilde{z}_{k+j}\tilde{z}_k^T]$ in Eq. (34). Then, the following formula can be obtained:

$$\begin{bmatrix} P_{k/k-1} & C_{k/k-1} \\ C_{k/k-1}^T & P_{pp} \end{bmatrix} \begin{bmatrix} H_k^T \\ N_k^T \end{bmatrix} - \bar{K}_k V_k = 0 \tag{37}$$

Substituting the Eq. (22) into the Eq. (37) can be obtained:

$$[H_k, N_k] \begin{bmatrix} P_{k/k-1} & C_{k/k-1} \\ C_{k/k-1}^T & P_{pp} \end{bmatrix} \begin{bmatrix} H_k^T \\ N_k^T \end{bmatrix} = V_k - R_k \tag{38}$$

Expanding the above augmented formula

$$[H_k, N_k] \left(S_{k/k-1} + \begin{bmatrix} Q_{k-1} & 0 \\ 0 & 0 \end{bmatrix} \right) \begin{bmatrix} H_k^T \\ N_k^T \end{bmatrix} = V_k - R_k \tag{39}$$

where

$$S_{k/k-1} = \begin{bmatrix} \lambda_k P_{k/k-1}^* & (\Phi_{k/k-1} C_{k-1} + \Psi_{k/k-1} P_{pp}) \\ (\Phi_{k/k-1} C_{k-1} + \Psi_{k/k-1} P_{pp})^T & P_{pp} \end{bmatrix} \tag{40}$$

Substituting and transposing the formula

$$[H_k, N_k] S_{k/k-1} \begin{bmatrix} H_k^T \\ N_k^T \end{bmatrix} = V_k - H_k Q_{k-1} H_k^T - R_k \tag{41}$$

and then

$$\begin{aligned} &\lambda_k H_k P_{k/k-1}^* H_k^T \\ &\quad = V_k - H_k Q_{k-1} H_k^T - N_k P_{pp} N_k^T - R_k \\ &\qquad - N_k \left(\Phi_{k/k-1} C_{k-1} + \Psi_{k/k-1} P_{pp}\right)^T H_k^T \\ &\qquad - H_k \left(\Phi_{k/k-1} C_{k-1} + \Psi_{k/k-1} P_{pp}\right) N_k^T \end{aligned} \tag{42}$$

Taking traces on both sides of Eq. (42), and simplifying the formula

$$\lambda_k Tr(M_k) = Tr(O_k) \tag{43}$$

where,

$$\begin{aligned} O_k &= V_k - N_k(\Phi_{k/k-1} C_{k-1} + \Psi_{k/k-1} P_{pp})^T H_k^T \\ &\quad - H_k(\Phi_{k/k-1} C_{k-1} + \Psi_{k/k-1} P_{pp}) N_k^T \\ &\quad - H_k Q_{k-1} H_k^T - N_k P_{pp} N_k^T - R_k \end{aligned} \tag{44}$$

$$M_k = H_k P_{k/k-1}^* H_k^T \tag{45}$$

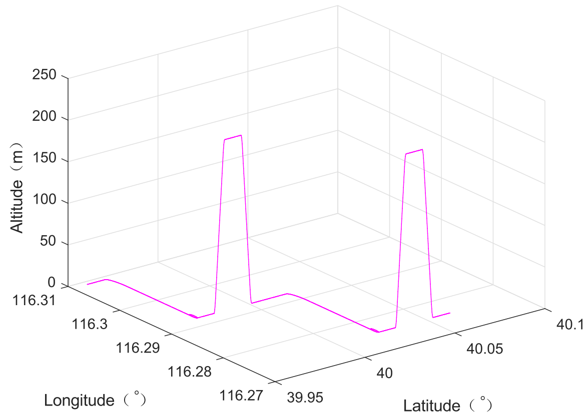

FIGURE 1. Vehicle trajectory.

Then, the suboptimal adaptive fading factor can be determined by the following formula:

$$c_k = \frac{Tr(O_k)}{Tr(M_k)} \tag{46}$$

$$\lambda_k = \begin{cases} c_k, & c_k \geq 1 \\ 1, & c_k < 1 \end{cases} \tag{47}$$

where the residual sequence V_k in Eq. (44) can be obtained:

$$V_k = \begin{cases} \tilde{z}_1 \tilde{z}_1^T, & k = 1 \\ \dfrac{\rho V_{k-1} + \tilde{z}_k \tilde{z}_k^T}{1 + \rho}, & k > 1 \end{cases} \tag{48}$$

where $0 < \rho \leq 1$ is a forgetting factor, and usually $\rho = 0.95$.

By using the above fading factor λ_k, the predicted state error covariance $P_{k/k-1}$ is modified, the gain matrix K_k is adjusted, and the predicted measurement residual sequences satisfies the mutually orthogonal principle. From the above derivation, the procedure of the proposed PSTECKF algorithm is summarized in Table 1.

V. NUMERICAL SIMULATION

To evaluate the performance of the proposed PSTECKF for the INS/GNSS integrated navigation system of a UAV, a numerical simulation has been carried out. The ECKF and EKF algorithms for the navigation system are selected to compare with the proposed PSTECKF.

In simulation, the trajectory of the UAV is shown in Fig.1, in which climb, fall, turn and shifting motions are implemented in the flight path. The simulation parameters are shown in Table 2, and the data for the INS and GNSS error specifications are listed in Table 3. The sampling period of INS is 0.01s, the sampling period and filtering period of GNSS are 1s, and the total simulation time is 1932s.

In order to evaluate the performance of the EKF, ECKF and PSTECKF algorithms under model uncertainties, the

TABLE 1. Implementation algorithm for PSTECKF.

Step 1: Initialization: Initialize state $\hat{x}_0$, state covariance matrix P_0 and cross-covariance variance $C_0 = 0$

Step 2: Time update

1) Predict state

$$\hat{x}_{k/k-1} = f(\hat{x}_{k-1}, \bar{p}) \tag{49}$$

2) Predict observation

$$\hat{z}_k = h(\hat{x}_{k/k-1}, \bar{p}) \tag{50}$$

3) Calculate suboptimal adaptive fading factor

$$\lambda_k = \begin{cases} c_k, c_k \geq 1 \\ 1, c_k < 1 \end{cases} \tag{51}$$

4) Predict state covariance matrix

$$P_{k/k-1} = \lambda_k P^*_{k/k-1} + Q_{k-1} \tag{52}$$

where $P^*_{k/k-1} = \Phi_{k/k-1} P_{k-1} \Phi^T_{k/k-1} + \Phi_{k/k-1} C_{k-1} \Psi^T_{k/k-1} + \Psi_{k/k-1} C^T_{k-1} \Phi^T_{k/k-1} + \Psi_{k/k-1} P_{pp} \Psi^T_{k/k-1}$.

5) Predict cross-covariance matrix

$$C_{k/k-1} = \Phi_{k/k-1} C_{k-1} + \Psi_{k/k-1} P_{pp} \tag{53}$$

where

$$c_k = \frac{Tr(O_k)}{Tr(M_k)} \tag{54}$$

$$\begin{aligned} O_k = V_k &- N_k \left(\Phi_{k/k-1} C_{k-1} + \Psi_{k/k-1} P_{pp}\right)^T H_k^T \\ &- H_k \left(\Phi_{k/k-1} C_{k-1} + \Psi_{k/k-1} P_{pp}\right) N_k^T - H_k Q_{k-1} H_k^T - N_k P_{pp} N_k^T - R_k \end{aligned} \tag{55}$$

$$M_k = H_k P^*_{k/k-1} H_k^T \tag{56}$$

Step 3: Measurement update

6) Calculate gain matrix

$$K_k = (P_{k/k-1} H_k^T + C_{k/k-1} N_k^T)(H_k P_{k/k-1} H_k^T + N_k C^T_{k/k-1} H_k^T + H_k C_{k/k-1} N_k^T + N_k P_{pp} N_k^T + R_k)^{-1} \tag{57}$$

7) Estimate state

$$\hat{x}_k = \hat{x}_{k/k-1} + K_k \{z_k - h(\hat{x}_{k/k-1}, \bar{p})\} \tag{58}$$

8) Calculate state covariance matrix

$$P_k = (I - K_k H_k) P_{k/k-1} - K_k N_k C^T_{k/k-1} \tag{59}$$

9) Calculate cross-covariance matrix

$$C_k = (I - K_k H_k) C_{k/k-1} - K_k N_k P_{pp} \tag{60}$$

TABLE 2. Simulation parameters in the EKF, ECKF and PSTECKF.

Parameter	Value
Initial position	$(116.31°, 39.96°, 3m)$
Initial velocity	$(0m/s, 0m/s, 0m/s)$
Initial orientation	$(0°, 0°, 0°)$
Initial position error	$(0°, 0°, 0m)$
Initial velocity error	$(0.1m/s, 0.1m/s, 0.1m/s)$
Initial attitude error	$(-0.0001°, 0.0001°, -0.0058°)$

TABLE 3. INS and GNSS error specifications.

Sensor	Range	Value
Gyro parameters	Constant drift	$0.03(°)/h$
	White noise	$0.001(°)/h$
	Sampling rate	$100Hz$
Accelerometer parameters	Zero bias	$10^{-4}g$
	White noise	$10^{-5}g$
	Sampling rate	$100Hz$
GNSS receiver parameters	RMSE of horizontal position	$8m$
	RMSE of altitude	$4m$
	RMSE of velocity	$0.3m/s$
	Sampling rate	$1Hz$

process noises, the measurement noises, the state perturbations and the measurement biases are added into the simulations. The measurement biases distributed to a normal distribution, which has mean zeros and covariance $diag\left[0.1m/s, 0.1m/s, 0.9m/s, (10^{-6})°, (10^{-8})°, 5m\right]$.

The dynamic model is added into the state perturbations during two time intervals, which are from 400s to 700s and

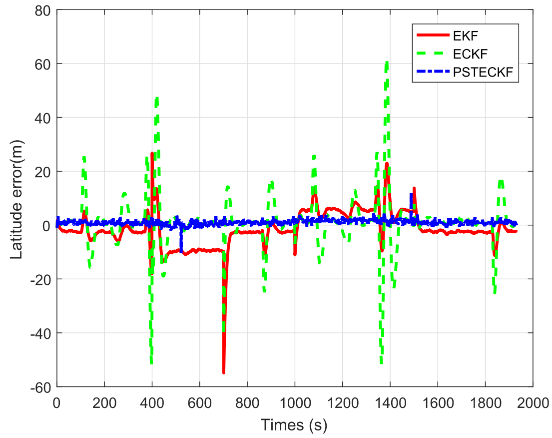

FIGURE 2. Latitude error.

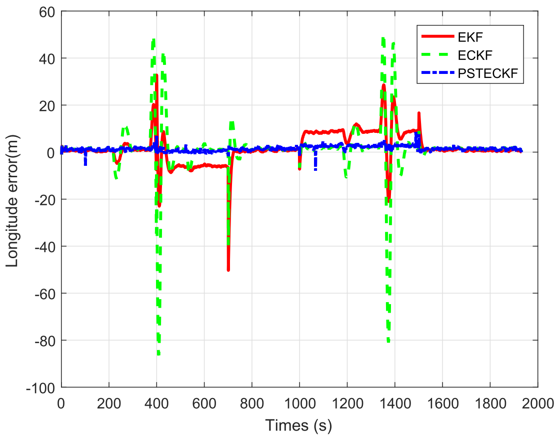

FIGURE 3. Longitude error.

from 1000s to 1500s, and the values are given by

$$\Delta x = \begin{cases} [0_{1\times 15}]^T, \\ 0 < t < 400 or 700 < t < 1000 or t > 1500 \\ [0_{1\times 3}, 0.5, 0.5, 0.5, 50/Re, 50/Re, 50, 0_{1\times 6}]^T, \\ 400 \leq t \leq 700 \\ [0_{1\times 3}, -[0.8, 0.8, 0.8], -10/Re, -10/Re, -10, 0_{1\times 6}]^T, \\ 1000 \leq t \leq 1500 \end{cases} \tag{61}$$

under the above condition, the EKF, ECKF and PSTECKF algorithms are used in the INS/GNSS integrated navigation simulations of the UAV. The position errors and velocity errors of the above three filters are listed in Figures 2-7, respectively.

From Figs. 2-4, it can be seen that the position estimation errors of the EKF is off zeros because of the biases in the INS/GNSS integrated navigation system, in which the altitude errors are the biggest. The position errors of the ECKF fluctuate around zeros, because the ECKF combines the statistics of biases into the state estimation formula by using the "consider" method and mitigates the negative effects of the biases. But, when the UAV is maneuvering, these errors

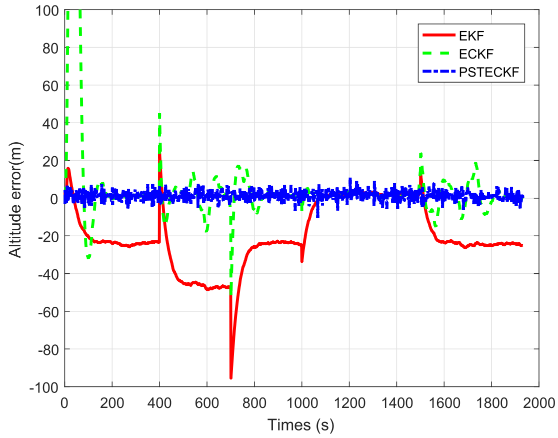

FIGURE 4. Altitude error.

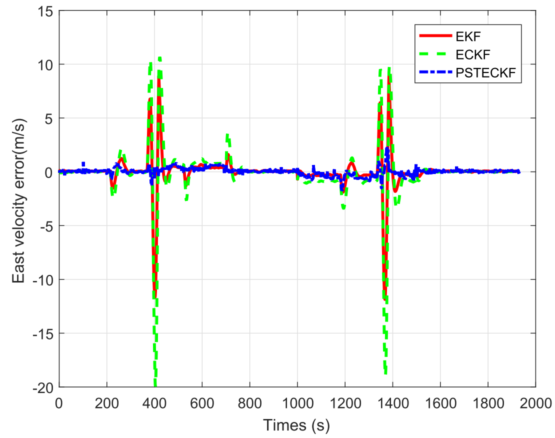

FIGURE 5. East velocity error.

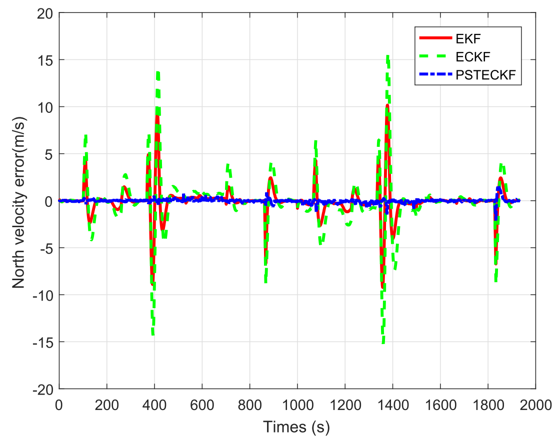

FIGURE 6. North velocity error.

of the ECKF are bigger than the errors of the EKF on account of the nonlinear approximation errors coming from the Taylor expansion and Jacobi matrices, and the overcompensation of the bias covariance. The position errors of the PSTECKF are smallest in three results by introducing the adaptive factor to reduce the nonlinear approximation errors and the perturbations of navigation system.

Similar results emerged in the state estimation of the velocity of the integrated navigation in Figs. 5-7. For the up

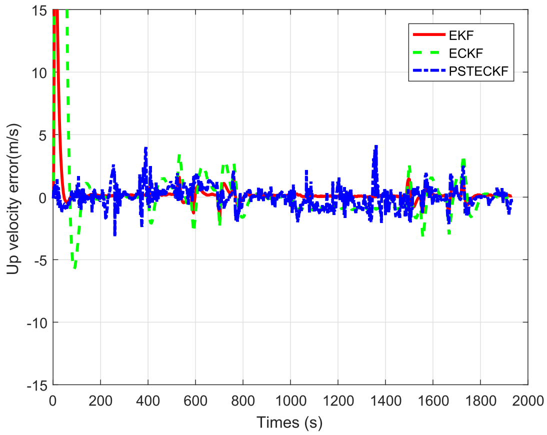

FIGURE 7. Up velocity error.

velocity in Fig. 7, the errors of the EKF have a bias about 2m/s, the errors of the ECKF have big fluctuation and also have a bias of dynamic state disturbance during 400s to 700s and 1000s to 1500s, and the errors of the PSTECKF fluctuate around zeros with a bigger covariance respected with the EKF and ECKF. For the east velocity in Fig. 5 and the north velocity in Fig. 6, the errors of the PSTECKF are the smallest, and the errors of the ECKF are the biggest for the same reason in the position.

The above simulations and analyses demonstrate that the proposed PSTECKF can effectively mitigate the negative effects of the biases and perturbations of the integrated navigation system, and has a better navigation performance than the EKF and the ECKF in totally.

VI. CONCLUSION

By considering the biases and perturbations in the INS/GNSS integrated navigation system, the novel partially strong tracking extended consider Kalman filtering (PSTECKF) is proposed to mitigate the negative effects of these uncertainties. Comparing with the extended Kalman filtering (EKF), the proposed PSTECKF makes two main changes. One change is considering the biases and incorporating their covariance into the state error covariance and the Kalman gain matrices to balance the state estimation and the measurements, but not estimates these biases. Another is partially introducing the adaptive fading factor into the predicted covariance of the states, which are not all the augmented states, to compensate the nonlinear approximation errors and some covariance uncertainties. Numerical simulations for the INS/GNSS integrated navigation of the unmanned aerial vehicle demonstrate the effectiveness of the proposed PSTECKF in terms of mitigating the biases and perturbations in navigation system compared to the EKF and the extended consider Kalman filtering.

REFERENCES

[1] P. D. Groves, *Principles of GNSS, Inertial, and Multisensor Integrated Navigation Systems*. Norwood, MA, USA: Artech House, 2013.

[2] S. Gao, L. Xue, Y. Zhong, and C. Gu, "Random weighting method for estimation of error characteristics in SINS/GPS/SAR integrated navigation system," *Aerosp. Sci. Technol.*, vol. 46, pp. 22–29, Oct./Nov. 2015.

[3] M. Fu, Z. Deng, and J. Zhang, *Kalman Filtering Theory and Its Application in Navigation System*, 2nd ed. Beijing, China: Science Press, 2010.

[4] J. L. Crassidis, "Sigma-point Kalman filtering for integrated GPS and inertial navigation," *IEEE Trans. Aerosp. Electron. Syst.*, vol. 42, no. 2, pp. 750–756, Apr. 2006.

[5] J. Farrell and M. Barth, *The Global Positioning System & Inertial Navigation*, vol. 61. New York, NY, USA: McGraw-Hill, 1999.

[6] Y. Qin, H. Zhang, and S. Wang, *Kalman Filtering and Integrated Navigation Principle*. Xi'an, China: Northwestern Polytechnical Univ. Press (in Chinese), 1998.

[7] B. Yang, Y. Qin, and Y. Chai, "Application of UKF in direct method of Kalman filter for INS/GPS," *Chin. J. Sens. Actuators*, vol. 20, no. 4, pp. 842–846, 2007.

[8] Y. Meng, S. Gao, Y. Zhong, G. Hu, and A. Subic, "Covariance matching based adaptive unscented Kalman filter for direct filtering in INS/GNSS integration," *Acta Astron.*, vol. 120, pp. 171–181, Mar. 2016.

[9] G. Hu, W. Wang, Y. Zhong, B. Gao, and C. Gu, "A new direct filtering approach to INS/GNSS integration," *Aerosp. Sci. Technol.*, vol. 77, pp. 755–764, Jun. 2018.

[10] S. S. Ren, L. Y. Zhao, and T. S. Lou, "A strong tracking SDRE filter for GPS /INS integrated navigation," *J. Projectiles, Rockets, Missiles Guid.*, vol. 37, no. 5, pp. 43–46 and 55, 2017.

[11] J. L. Crassidis and J. L. Junkins, *Optimal Estimation of Dynamic Systems*, 2nd ed. Boca Raton, FL, USA: CRC Press, 2012, pp. 231–238.

[12] F. Sun and L. Tang, "Improved particle filter algorithm for INS/GPS integrated navigation system," in *Proc. IEEE Int. Conf. Mechatronics Autom.*, Beijing, China, Aug. 2011, pp. 2392–2396.

[13] C. Tseng, S. Lin, and D. Jwo, "Fuzzy adaptive cubature Kalman filter for integrated navigation systems," *Sensors*, vol. 16, no. 8, p. 1167, Aug. 2016.

[14] D.-J. Jwo, C.-F. Yang, C.-H. Chuang, and T.-Y. Lee, "Performance enhancement for ultra-tight GPS/INS integration using a fuzzy adaptive strong tracking unscented Kalman filter," *Nonlinear Dyn.*, vol. 73, no. 1, pp. 377–395, 2013.

[15] M. Liu and F. Xiong, "A fuzzy adaptive GPS/INS integrated navigation algorithm," *Procedia Eng.*, vol. 15, pp. 660–664, Jan. 2011.

[16] K. H. Kim, J. G. Lee, and C. G. Park, "Adaptive two-stage extended Kalman filter for a fault-tolerant INS-GPS loosely coupled system," *IEEE Trans. Aerosp. Electron. Syst.*, vol. 45, no. 1, pp. 125–137, Jan. 2009.

[17] M. George and S. Sukkarieh, "Tightly coupled INS/GPS with bias estimation for UAV applications," in *Proc. Austral. Conf. Robot. Automat. (ACRA)*, Sydney, NSW, Australia, 2005, pp. 1–7.

[18] L. Zhao, H. Qiu, and Y. Feng, "Analysis of a robust Kalman filter in loosely coupled GPS/INS navigation system," *Measurement*, vol. 80, pp. 138–147, Feb. 2016.

[19] S. F. Schmidt, "Application of state-space methods to navigation problems," *Adv. Control Syst.*, vol. 3, pp. 293–340, Jan. 1996.

[20] T. Lou, H. Fu, Y. Zhang, and Z. Wang, "Consider unobservable uncertain parameters using radio beacon navigation during Mars entry," *Adv. Space Res.*, vol. 55, no. 4, pp. 1038–1050, 2015.

[21] T. Lou, "Research on self-calibration filtering method of the dynamic model and measurement model during Mars entry," Ph.D. dissertation, Beihang Univ., Beijing, China, 2015.

[22] S. Zhang, Y. Bar-Shalom, and G. Watson, "Tracking with multisensor out-of-sequence measurements with residual biases," in *Proc. 13th Int. Conf. Inf. Fusion*, Edinburgh, U.K., Jul. 2010, pp. 1–8.

[23] J. S. McCabe, "Multitarget tracking and terrain-aided navigation using square-root consider filters," Ph.D. dissertation, Missouri Univ. Sci. Technol., Rolla, MO, USA, 2018.

[24] S. A. Chee and J. R. Forbes, "Norm-constrained consider Kalman filtering," *J. Guid., Control, Dyn.*, vol. 37, no. 6, pp. 1–5, 2014.

[25] T.-S. Lou, N.-H. Chen, H. Xiong, Y.-X. Li, and L. Wang, "Ensemble consider Kalman filtering," 2019, *arXiv:1906.06695*. [Online]. Available: https://arxiv.org/abs/1906.06695

[26] J. Stauch and M. Jah, "Unscented Schmidt–Kalman filter algorithm," *J. Guid., Control, Dyn.*, vol. 38, no. 1, pp. 117–123, 2014.

[27] T.-S. Lou, Z.-H. Wang, M.-L. Xiao, and H.-M. Fu, "Multiple adaptive fading Schmidt–Kalman filter for unknown bias," *Math. Problems Eng.*, vol. 2014, Nov. 2014, Art. no. 623930.

[28] J. S. McCabe and K. J. DeMars, "The Gaussian mixture consider Kalman filter," in *Proc. AAS/AIAA 25th Space Flight Mech. Meeting*, Williamsbug, VA, USA, 2016.

[29] W. Quan, J. Li, X. Gong, and J. Fang, *INS/CNS/GNSS Integrated Navigation Technology*. Berlin, Germany: Springer, 2015.

[30] H. Qi and J. B. Moore, "Direct Kalman filtering approach for GPS/INS integration," *IEEE Trans. Aerosp. Electron. Syst.*, vol. 38, no. 2, pp. 687–693, Apr. 2002.

[31] D. H. Zhou and P. M. Frank, "Strong tracking filtering of nonlinear time-varying stochastic systems with coloured noise: Application to parameter estimation and empirical robustness analysis," *Int. J. Control*, vol. 65, no. 2, pp. 295–307, Oct. 1996.

[32] D. H. Zhou, Y. G. Xi, and Z. J. Zhang, "A suboptimal multiple fading extended Kalman filter," *Acta Automatica Sinica China*, vol. 17, no. 6, pp. 689–695, 1999.

TAI-SHAN LOU received the Bachelor of Science degree in mathematics and applied mathematics, the master's degree in applied mathematics, and the Ph.D. degree in engineering mechanics from Beihang University, Beijing, China, in 2003, 2009, and 2015, respectively. He is currently a Lecturer with the School of Electrical and Information Engineering, Zhengzhou University of Light Industry. He has published and coauthored more than 30 articles in both national and international publications. His main research interests are filtering theory, control theory, navigation, and data fusion.

NAN-HUA CHEN was born in Henan, China, in 1994. He received the bachelor's degree in automation from the Zhengzhou University of Light Industry, in 2016, where he is currently pursuing the master's degree in testing technology and automation equipment. His main research interests include Kalman filter, integrated navigation, and UAV.

ZHI-WU CHEN was born in Henan, China, in 1976. He received the master's degree from the Harbin Institute of Technology. He is currently an Associate Professor with the Department of Automation, School of Electrical and Information Engineering, Zhengzhou University of Light Industry. His main research interest includes modern complex industrial network control systems. He has published more than ten articles; he has guided students to participate in national and provincial competitions and won awards.

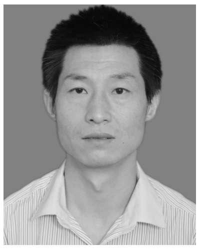

XIAO-LEI WANG received the bachelor's degree in computer information and management from Hebei University, Baoding, China, in 2004, the master's degree in agricultural mechanical engineering from Henan Agricultural University, Zhengzhou, China, in 2009, and the Ph.D. degree in instrument science and technology from Southeast University, Nanjing, China, in 2014. He is currently a Lecturer with the School of Electrical and Information Engineering, Zhengzhou University of Light Industry. He has published more than 20 articles in both national publications and international conference. His main research interests include sensor technology, measurement control technology, navigation measurement and control systems, and data fusion.